

STRUCTURAL AND MAGNETIC PROPERTIES OF NANOPERTICULATED Fe-SnO_x SYSTEMS

P. C. Cajas, patolacajas@gmail.com

Faculty of Technology, Department of Mechanical Sciences, University of Brasília, Brasília, Brazil

F. H. Aragón, fermin964@hotmail.com

J. A. H. Coaquira, coaquira@unb.br

Institute of physics, University of Brasília, Brasília, Brazil

J. E. Rodríguez-Páez, jnpaez60@yahoo.com

Group CYTEMAC. Department of Physics, University of Cauca, Popayán – Colombia

Abstract. We successfully synthesized SnO₂ and SnO nanoparticles doped with 8 mol% Fe by the controlled precipitation method. X-ray diffraction technique has been used to identify the crystalline phases and estimate the crystallite size. Raman spectroscopy has been used to evaluate the size and doping effects on the vibrational properties. The results indicate that the substitution of tin by iron atoms occurs likely in a solid solution regime. The magnetic properties of the SnO_x-Fe compounds were determined by the magnetization dependence on temperature and magnetic field. The low-field magnetization as a function of the temperature curves: zero-field cooled (ZFC) and field-cooled (FC) curves show features consistent with the thermal activation of blocked magnetic moments of superparamagnetic particles. The hysteresis curves showed coercive fields of ~200 Oe (cassiterite) and ~300 Oe (romarchite) at 5K, meanwhile at 300 K the coercive field of both compounds practically disappears. The absence of coercive field at high temperatures is in agreement with the thermal relaxation of superparamagnetic particles.

Keywords: Synthesis, controlled precipitation method, SnO_x-Fe; nanoparticles, magnetic properties

1. INTRODUCTION

One of the tin oxide compounds, the romarchite (SnO) has a blue-black color and it is soluble in common acids and strong bases. SnO is commonly used in the synthesis of stannous salts, electroplating, etc. SnO compounds stabilized in the tetragonal structure with a space group $p/4nmm$. Its fusion temperature is 1080°C and its density is 134.71 g/mol (A. Mosquera 2008). On the other hand, the cassiterite phase (SnO₂), is a white crystalline powder and insoluble in acids. SnO₂ is used in the manufacture of electrodes (Freddy Dante 2005), gas sensors (A. Montenegro 2007) and varistors (A. Mosquera 2007). The SnO₂ has a tetragonal structure of rutile type with a space group $p/4_2mnm$ and lattice parameters $a = 4.737\text{Å}$ and $c = 3.186\text{Å}$ (Ararat-Ibarguen 2007). This compound is stable at high temperatures and resistant to chemical attack carried out with acids and bases.

Both tin oxide compounds are non-magnetic semiconductors (C. Rodriguez-Torres 2006). However, in order to induce magnetic properties the introduction of magnetic atoms into the structure is needed to obtain an oxide-diluted magnetic semiconductor (O-DMS). O-DMS systems with a Curie temperature above room temperature are wished in order to obtain the second generation of electronic devices in "spintronic" (Rubi Diego 2006), in applications such as optoelectronic and magnetoelectric devices (Coe 2007), magnetic gas sensors etc.

Those tin oxide compounds can be produced by methods such as polymeric precursor (Pechini) (A. Mosquera 2008), controlled precipitation (Perez-Centeno 2008) and sol-gel (A. Montenegro 2009). Some authors have reported the production of SnO_x-Fe nanoparticles by mechanical alloying (C. Rodriguez 2005) and indicated the formation of Fe-doped SnO₂ nanoparticles with crystallite size of 15 nm, which show a room-temperature isothermal magnetization curve with a weak hysteresis. However, the 10-nm-sized crystals fabricated by a method called "polymeric complex method" show ferromagnetic behavior as the temperature is decreased (J. Sakuma 2007). Moreover, ⁵⁷Fe-doped SnO₂ nanoparticles with the ⁵⁷Fe content in the range of 0.5 - 15% and produced by the sol-gel method show, obtained paramagnetic behavior by Mössbauer spectroscopy (K. Nomura 2006).

In this work we present the study of SnO and SnO₂ nanoparticles doped with 8mol% Fe which were synthesized by a controlled precipitation method. That study consists on the characterization of the structural, vibrational and magnetic properties.

2. EXPERIMENTAL

SnO_x doped with 8 mol% Fe, were synthesized by the controlled precipitation method, using stannous chloride (Mallinckrod) as a tin precursor. It is worth mentioning that the used method allows one to obtain nanoparticles with appropriated morphology, permits one better control on the processes of powder synthesis and ensures good reproducibility. To promote the formation of cassiterite phase, a solution of water and ethanol in equal proportions was used as a solvent. On the other hand, romarchite phase was obtained using acetic acid as described in the literature (H. Avila 2009). The precipitations were obtained with a constant agitation (100 rpm) and an appropriate pH, which were monitored using a digital pH-meter (Metrohm Dosimat mark, reference 1.775.0010 No 061995). Preliminarily, in order to establish the appropriate pH values, the potentiometric titration curves was obtained for both systems. A pH=6.5 was established for the cassiterite precursor solution and a pH=8.0 for the romarchite precursor solution. To obtain the iron suspension, ferrous sulfate (Mallinckrod) was dissolved in deionized water and adjusting the pH=8. Finally, the Sn and Fe precursor solutions were mixed and aged for 24 hours. Several washing procedures were made with a dietilamine (0.1M) solution in order to eliminate the remaining chlorides and/or sulfates in the system. The final powders were thermal treated for 24 h at 100 °C to guarantee the particle size stabilization and thermodynamic equilibrium of the dopant distribution. In order to determine the crystalline phase and estimate the crystallite size a X-ray diffraction apparatus (Bruker diffractometer) with Cu $K\alpha$ radiation has been used. The 2θ scanning range from 20° to 90° and a step size of 0.02° was used. Room-temperature Raman spectroscopy measurements (Jovin Yvon-Spex T64000) were carried out using the green line (wavelength, 514 nm) of an Ar laser excitation source.

The magnetic properties of SnO_x -Fe compounds were determined using a commercial Vibrating Sample Magnetometer (PPMS, Quantum Design). Those magnetic measurements were obtained in the temperature range of 5 to 300 K and with applied magnetic fields up to 90 kOe.

3. RESULTS AND DISCUSSION

3.1 Structural characterization

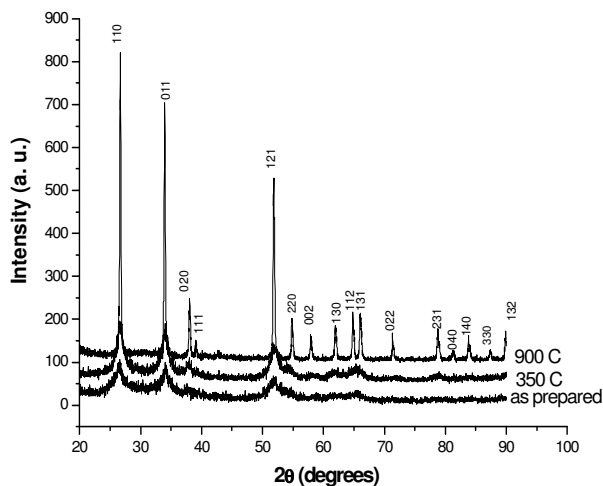


Figure 1. XRD patterns of the Fe-doped SnO_2 powder with 8 mol% Fe. The lower pattern corresponds to the as-synthesized powder; the middle pattern corresponds to the powder treated at 350 °C for one hour and the top pattern corresponds to the powder treated at 900 °C for one hour.

In Figure 1 is shown the XRD diffraction patterns of the synthesized powders. Pattern of the as-prepared sample shows broad and poorly defined reflections of cassiterite phase (PDF41-1445), which suggests that the structure is not fully crystallized. After the thermal treatment at 350 °C and 900 °C the reflections become sharper as the temperature is increased. This result indicates that the thermal treatment favors the sample crystallization as higher temperatures drive to sharper reflections. Using the Scherrer relation an average crystallite size of ~5 nm has been estimated from the as-prepared sample and that crystallite size goes to 4nm and 52nm for the thermal treated samples at 350 and 900 C, respectively.

On the other hand, the procedure used to promote the formation of the romarchita phase (using acetic acid solvent) provides powders where the coexistence of two crystalline phases (SnO and SnO₂) has been determined, where the SnO (PDF01-0902) is the main phase (~89%) and SnO₂ (PDF41-1445) is the secondary phase (~11%).

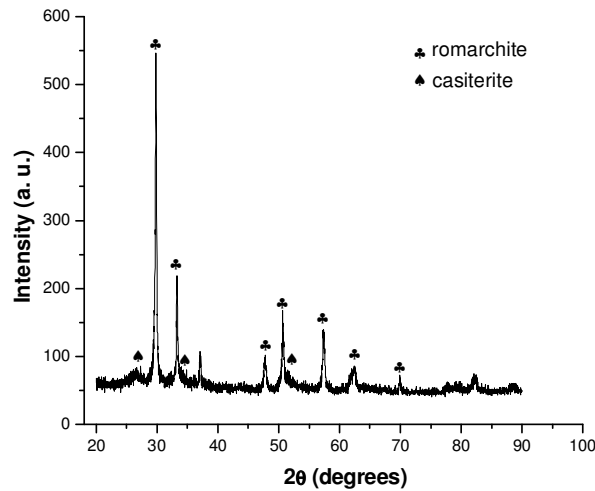


Figure 2. X-ray diffraction pattern of the as-prepared tin oxide powder obtained by using acetic acid as solvent with pH=8 and doped with 8 mol% Fe.

As shown in figure 2, the X-ray pattern of as-prepared sample indicates that the SnO phase shows sharper reflections which can be associated to better crystallization. Since sharper reflections means better crystallization and larger crystallite size, the as-prepared romarchite phase shows larger crystallite size (~45 nm) than the as-prepared cassiterite phase (~5 nm).

3.2. Raman Spectroscopy

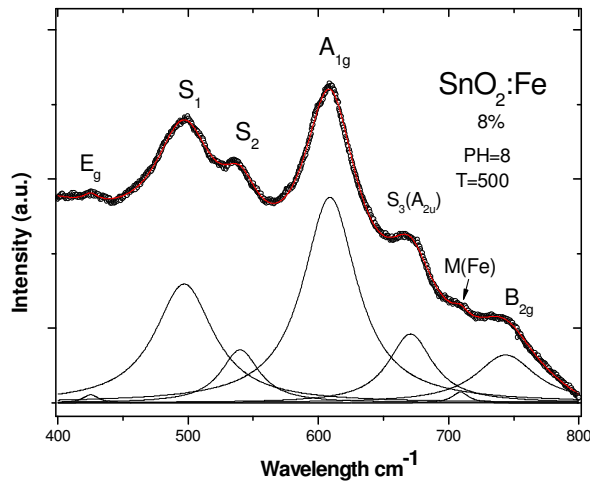


Figure 3. Room-temperature Raman spectrum of the Fe-doped SnO₂ powder doped with 8%mol Fe and thermally treated at 500 °C.

In figure 3 is shown the Raman spectrum of Fe-doped SnO₂ with 8 mol% Fe and thermally treated at 500 C. The experimental data were fitted to lorentzian-shape peaks. From that analysis were determined classical modes (E_g, A_{1g}, B_{2g}) of the cassiterite phase (O. Lupan, et al. 2009). Besides those modes, unexpected modes called S₁, S₂ and S₃ were determined. Based on previous report (F. H. Aragón et al. 2010) the S₁ and S₂ bands were associated to the disorder-activated modes located at the particles. The S₃ mode must be related to the A_{2u} mode which seems to be activated by the confinement effect. The peak located at 723 cm⁻¹, not observed in undoped SnO₂ samples has been associated with

the local vibrational mode of iron atoms (M. N. Rumyantseva, et al. 2005) substituting Sn atoms in the SnO₂ matrix. The latter result suggests that the Fe atoms are uniformly distributed on the whole particle (a solid-solution regime).

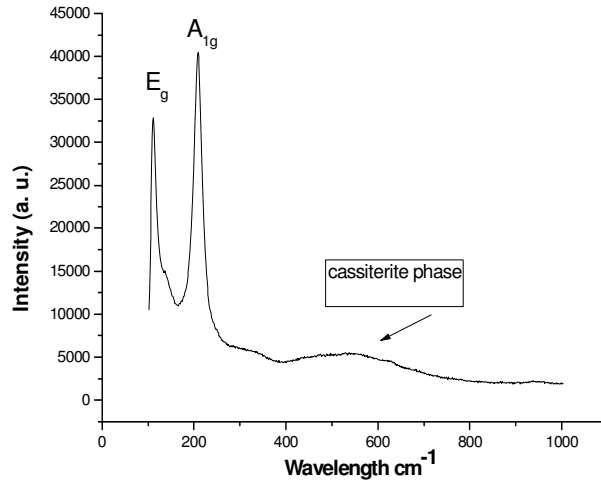


Figure 4. Raman spectrum of the sample doped with 8 mol% Fe and synthesized with acetic acid where the romarchite phase is the main phase (the sample was thermally treated at 350 °C).

Figure 4 shows the Raman spectrum of the sample doped with 8 mol% Fe and synthesized with acetic acid. As observed, sharp peaks were determined which were assigned to classical modes E_g and A_{1g} of romarchite structure (X. Wang, et al, 2004). The positions of those modes are at 165 cm⁻¹ and 220 cm⁻¹, respectively. Other weak modes near to classical modes are also observed, but their nature is not determined. Above 400 cm⁻¹, a broad band is observed. Since structural characterization indicates the presence of cassiterite phase in a small percentage, that broad band was associated with the modes of the cassiterite phase.

3.3. Magnetic properties

- Low-field magnetization curves

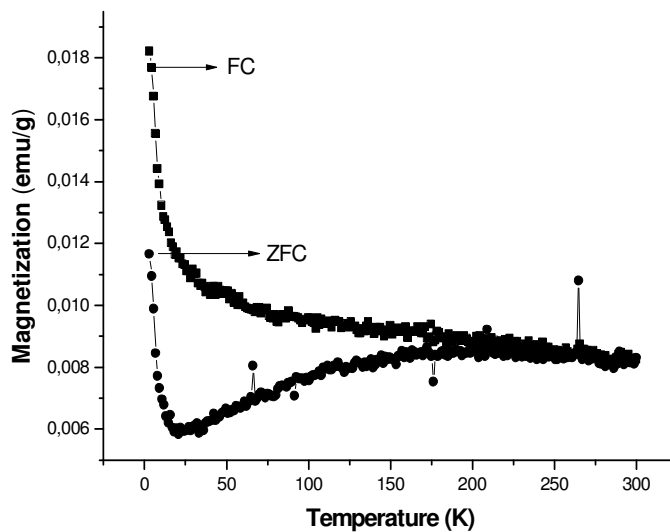


Figure 5. Zero-field-cooled (ZFC) and field-cooled (FC) curves as a function of the temperature obtained at H=100 Oe for the Fe-doped SnO₂ powders doped with 8 mol% Fe and thermally treated at 500 °C.

In figures 5 and 6 are shown the zero-field-cooled (ZFC) and field-cooled (FC) traces obtained at $H=100$ Oe for the $\text{SnO}_x\text{-Fe}$ nanoparticulated systems which were thermally treated, the SnO_2 at 500°C and SnO at 350°C . As can be observed in figure 5 the Fe-doped SnO_2 sample shows features consistent with a magnetic-thermal relaxation process. The ZFC traces show a broad maximum at ~ 200 K, which was associated with the freezing temperature, and the irreversibility between ZFC and FC traces starts above that maximum at ~ 250 K. The strong increasing tendency observed in the low-temperature region as the temperature is decreased must be associated with a paramagnetic contribution coming from extrinsic impurities or extremely small particles or paramagnetic clusters which are not detected by XRD experiments due to its detection limit. That paramagnetic contribution is better observed as the strength of the magnetic field is increased (data not shown).

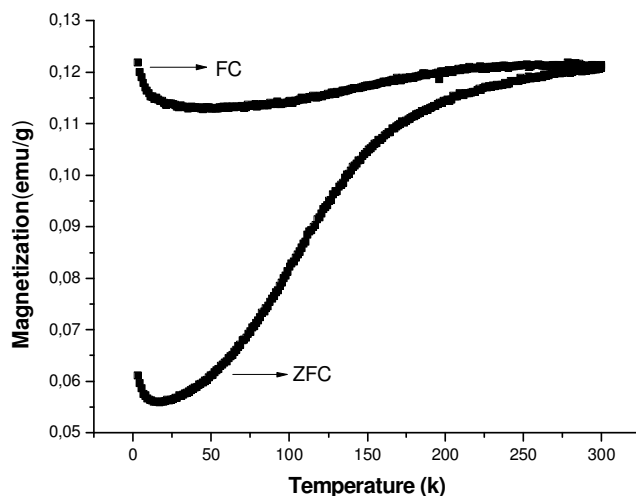


Figure 6. Zero-field-cooled (ZFC) and field-cooled (FC) curves as a function of the temperature obtained at $H=100$ Oe for the Fe-doped SnO powders doped with 8 mol% Fe and thermally treated at 350°C .

On the other hand, low-field magnetization curves of the Fe-doped SnO sample similar features. Irreversibility between the ZFC and FC traces is observed in the region below ~ 280 K and the maximum of the ZFC curve seems to be located above 300 K. It suggests us that the blocking process happens at higher temperatures in comparison with that observed for Fe-doped SnO_2 sample, likely because of the larger particle size determined for the Fe-doped SnO sample. Other remarkable feature can be observed in the low-temperature region. The paramagnetic contribution is largely reduced in the Fe-doped SnO , which indicates a lesser population of extrinsic impurities or paramagnetic clusters or even extremely smaller particles than that one in Fe-doped SnO_2 .

- **Hysteresis curves**

In figure 7 is shown the magnetic isotherms (M vs. H) obtained at 5 and 300 K for the Fe-doped SnO_2 nanoparticles with 8 mol% Fe. Even though the absence of coercive field at 300 K, the tendency to saturation of the magnetization observed in the central region (low-field region) suggests the occurrence of particle-particle interactions which seem to survive well-above the blocking temperature. A coercive field $H_C \sim 210$ Oe and a remnant magnetization $M_R \sim 0.043$ emu/g is determined from the M vs. H curve obtained at $T=5$ K, although the contribution associated only with the thermally blocked moments (ferromagnetic behavior) is overwhelmed by the stronger paramagnetic contribution coming from extrinsic impurities or paramagnetic clusters. The paramagnetic contribution is largely reduced in the 300 K magnetic isotherm due to its temperature dependence (Curie law).

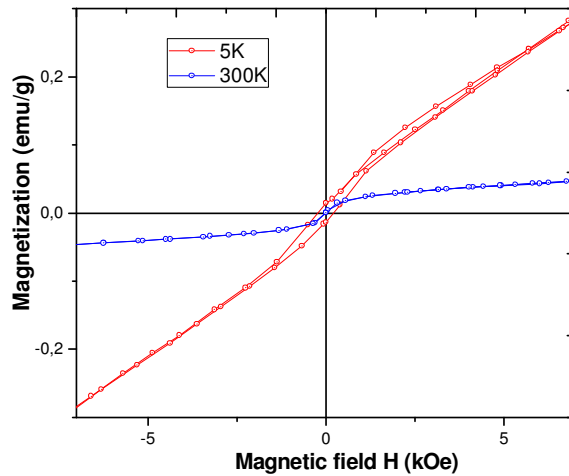


Figure 7. Magnetization as a function of the magnetic field obtained at 5 and 300K for the SnO₂ doped with 8 mol% Fe and thermally treated at 500°C.

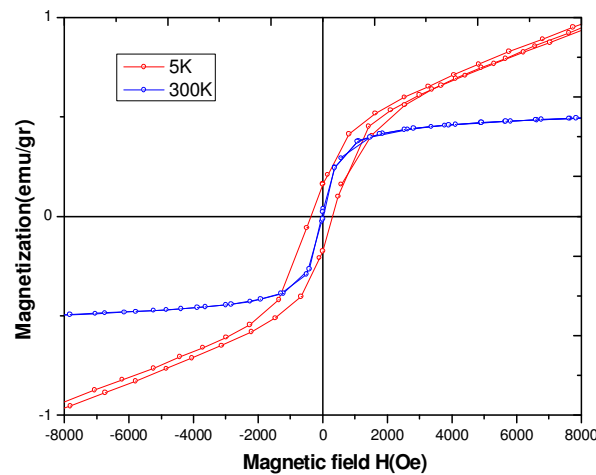


Figure 8. Magnetization as a function of the magnetic field obtained at 5 and 300K for the SnO doped with 8 mol% Fe, and thermally treated at 350°C.

On the other hand, the Fe-doped SnO sample shows larger coercive field at low temperatures as inferred in figure 8. A coercive field $H_C \sim 360$ Oe and a remnant magnetization of 0.167 emu/g is determined from the 5K-curve. Moreover, at room temperature the hysteresis curve gives almost zero coercive field. Those features are in agreement with a thermal blocking process. The increasing tendency of the magnetization above 2 kOe is associated with the paramagnetic contribution coming from extrinsic sources. At 300K, that paramagnetic contribution is absent due to its temperature dependence.

It is known that in SnO_x-Fe nanoparticulated systems the substitution of tin by iron ions produces defects mainly at the particle surface. Those defects (vacancies) play an important role since the ratio surface/volume is greatly enhanced due to the small particles size. Those vacancies must play an important role in the magnetic response of the system as determined in Ni-doped SnO₂ nanoparticles synthesized by a polymer precursor method (F. H. Aragon et al. 2010b). However, in order to determine the origin of the superparamagnetic behavior and its relation with the chemical bonds, particle size and content of dopant, additional characterizations are needed.

4. CONCLUSIONS

In this work, SnO and SnO₂ powders doped with 8 mol% Fe were synthesized using the controlled precipitation method. X-ray diffraction data analysis confirms the formation of the expected structure and provides the mean crystallite size of 5nm for the cassiterite and 45 nm for the romarchite compounds. The low-field magnetization measurements as a function of the temperature suggest the occurrence of the thermal activation of blocked magnetic moments of superparamagnetic particles and shows that the magnetic features depends on the particle size and chemical and structural properties. That blocking process is confirmed by the presence of coercive field in the magnetic isotherm at temperatures below the freezing temperature and the absence of that coercive field above that freezing temperature.

5. ACKNOWLEDGEMEST

Authors are grateful for the financial support of the Brazilian agencies CNPq and FAPDF. J.E.R.P. thanks to the University of Cauca for the financial support.

6. REFERENCES

A. Mosquera and J. E. Rodríguez-Páez 2008 “Obtención de nanoestructuras bidimensionales de SnO₂ utilizando el método de pechini: estudio de la conformación de la resina”, Boletín de la Sociedad Española de Cerámica y Vidrio, ISSN 0366-3175, Vol. 47, N°. 5, págs. 278-2.

A. Montenegro and Rodríguez-Páez 2009 “Síntesis óxido de estaño altamente reactivo utilizando como precursor etilhexanoato de estaño”, Revista Ingeniería e Investigación Vol. 29 No. 1, págs. (47-52).

A. Montenegro, et al. 2007 “SnO₂-Bi₂O₃ and SnO₂-Sb₂O₃, gas sensor, obtained by soft chemical method”, journal of the European Ceramic Society, Vol 2, pp. 4143-4146.

A. Mosquera, et al. 2007 “Syntesis of SnO₂ by Chemical Method, journal of the European Ceramic Society”, Vol 27 pp 3893-3896.

A. Mosquera and J. E. Rodríguez-Páez 2008 “Obtención de nanoestructuras bidimensionales de SnO₂ utilizando el método de pechini: estudio de la conformación de la resina”, Boletín de la Sociedad Española de Cerámica y Vidrio, ISSN 0366-3175, Vol. 47, N°. 5, págs. 278-286.

Ararat- et al. 2007 “Efecto de la naturaleza del precursor sobre las características de las nanopartículas de SnO₂ sintetizadas”, Quím. Nova vol.30 no.7 São Paulo.

A Pérez, et al. 2010 “Síntesis de nanoestructuras de SnO₂ y desarrollo de tecnología que permita caracterizar y controlar las etapas in situ de crecimiento”, universidad de Guadalajara, catálogo de servicios e investigación aplicada, U de G.

C. Rodriguez , et al. 2006 “Ferromagnetismo en películas delgadas de SnO₂ y Sn_{0.9}Fe_{0.1}O₂” Estudio experimental y de primeros principios, Villa de Merlo, San Luis - Libro de resúmenes AFA.

C. Rodríguez et al, “Magnetic behavior of nanoclusters of Fe -doped SnO₂”, Department de Physical- IFLP, Faculty C. Exactas, La Plata, Argentina.

D. Rubi 2006 “Nuevos Óxidos Metálicos Ferromagnéticos”, departamento de física, trabajo de grado, universidad autónoma de Barcelona.

F. H. Aragón 2010a “estudio de las propiedades estructurales y magnéticas de nanopartículas del SnO₂, dopadas con Ni, Co y Cr”, tesis de maestría del instituto de Física de la universidad de Brasilia – Brasil.

F. H. Aragón, et al, 2010 “Experimental study of the structural, microscopy and magnetic properties of Ni-doped SnO₂ nanoparticles”, J. Non-Crystalline Solids, 356, Issues 52-54, 2960-2964.

F. Dante, y Ojeda, 2005 “Oxidación anódica directa del tolueno sobre electrodos de SnO₂ dopado”, Huancayo – Perú.

H. Avila, and J. Rodríguez 2009, “Solvent effects in the synthesis process of the tin oxide”, J. Non-Cryst Sol, Vol. 355, pp 885-890.

J. Coey, et al. “Ferromagnetism in Fe-doped SnO₂ thin films” J.M. Physics Department, Trinity College, Dublin 2, Ireland, <<http://arxiv.org/ftp/cond-mat/papers/0401/0401293.pdf>>.

J. Sakuma, et al. 2007, “Mössbauer studies and magnetic properties of SnO₂ doped with ⁵⁷Fe”. Thin Solid Films 515, pp. 8653–8655.

K. Nomura, et al. 2006, “Mössbauer study of SnO₂ powders doped with dilute ⁵⁷Fe prepared by a sol-gel method”, J Phys 56, E 75.

M.N. Rumyantseva V. et al. 2005, “Nanocomposites SnO₂/Fe₂O₃: Wet chemical synthesis and nanostructure characterization”, Spain Available online 12 April.

O. Lupan ,et al. 2009, “Synthesis of one-dimensional SnO₂ nanorods via a hydrothermal technique”, physical E 41, pp 533-536.

X. Wang, et al. 2004, “infrared reflectivity, and Raman modes of SnO at high pressure”, phys. stat. sol. (b) 241, No. 14, 3168–3178.

7. RESPONSIBILITY NOTICE

The authors are the only responsible for the printed material included in this paper.